ChemComm

COMMUNICATION

View Article Online
View Journal | View Issue

Cite this: *Chem. Commun.*, 2023, 59, 12739

Received 1st August 2023,
Accepted 26th September 2023

DOI: 10.1039/d3cc03727d

rsc.li/chemcomm

Single crystal formation in core–shell capsules†

Marie Mettler,[a] Adrien Dewandre,[a] Nikolay Tumanov,[b] Johan Wouters[b] and Jean Septavaux *[a]

This work extends the scope of microfluidic-based crystallization methods by introducing solid microcapsules. Hundreds of perfectly similar microcapsules were generated per second, allowing a fast screening of crystallization conditions. XRD analyses were performed directly on encapsulated single crystals demonstrating the potential of this process for the characterization of compounds, including screening polymorphism.

Single-crystal X-ray diffraction (XRD) remains the preeminent method for the direct elucidation of molecular structures.[1] However, the formation of a suitable single crystal is challenging, with numerous parameters to be explored and materials in limited supply.[2] Several methods can be applied to reduce the nucleation rate in order to favour the formation of single crystals. Such crystallization methods have been used in chemistry labs for a very long time and include slow evaporation and vapor diffusion, cooling, solvent-induced crystallization, or crystallization from the melt, to cite some of the most common. More recent methods include crystallization under pressure, supercritical fluid crystallization or microfluidic crystallization, which uses microfluidic devices to control the flow of fluids and create small, uniform crystals. Besides, microfluidics also permits a tight control of diffusion parameters to control crystallisation phenomena,[3–5] or to prepare colloidal crystals[6] or crystal-like structures.[7]

Droplet microfluidics has emerged as a powerful tool for fast screening, particularly in drug discovery,[8] genomics[9] and crystallization.[10] It offers the advantage to produce, at high throughput (kHz), droplets of a few fLs to nLs surrounded by an immiscible phase, so that each droplet behaves like a small individual reactor that can contain biological material (cells,[11] DNA,[12] bacteria,[13] *etc.*) or chemical material.[8] For two decades, microfluidic-based approaches to single crystal formation, affording both low-scale experiments and screening capacities, have been extensively used for macromolecules and small molecules alike.[14–17] In this work, we propose a new approach based on the use of an emulsification generator capable of producing highly controlled double emulsions of core–shell type.[18] This system allowed us to produce microcapsules with an undersaturated liquid core confined in a solid polymer shell at a rate of several hundred capsules per second, each acting as an independent crystallization vessel.

To produce droplets in microfluidics, two immiscible fluids are sheared within structures of a typical size of 100 μm. Usual designs are T-junction, flow-focusing, co-flow or co-flow-focusing.[19] In the dripping[20] regime where the drop is formed close to the junction of the two fluids, highly monodisperse droplets (coefficient of variation CV < 2%) can be produced at frequencies up to several kHz. If a core–shell double emulsion is desired, a succession of two flow-focusing junctions can be used, but this requires the application of a combination of hydrophilic and hydrophobic surface treatments which makes this solution difficult to implement and not very durable over time.[21] Another solution is to use a device based on the use of aligned capillaries that do not require the use of surface treatments thanks to their cylindrical geometry, which prevents any contact between the emulsion and the wall of the extraction capillary. Utada *et al.* were the first to produce double emulsions using a capillary device.[22] In 2020, Dewandre *et al.* presented a new type of capillary-device (named Raydrop) based on the use of a 3D printed nozzle aligned with a collection capillary in a metallic cavity.[23] This design, described as non-embedded co-flow-focusing, has made it possible to manufacture a capillary device that is easy for non-experts to use. To produce double emulsions, an adapted nozzle that allows two fluids, the shell phase and the core phase, to be conveyed is used. These two fluids meet at the nozzle outlet, where the core phase is surrounded by the shell phase, which in turn is surrounded by the continuous phase filling the metal

[a] *Secoya Technologies Fond des Més 4, Louvain-la-Neuve 1348, Belgium. E-mail: jean.septavaux@secoya-tech.com*
[b] *Namur Institute of Structured Matter (NISM) Université de Namur, Rue de Bruxelles 61, Namur 5000, Belgium*

† Electronic supplementary information (ESI) available. See DOI: https://doi.org/10.1039/d3cc03727d

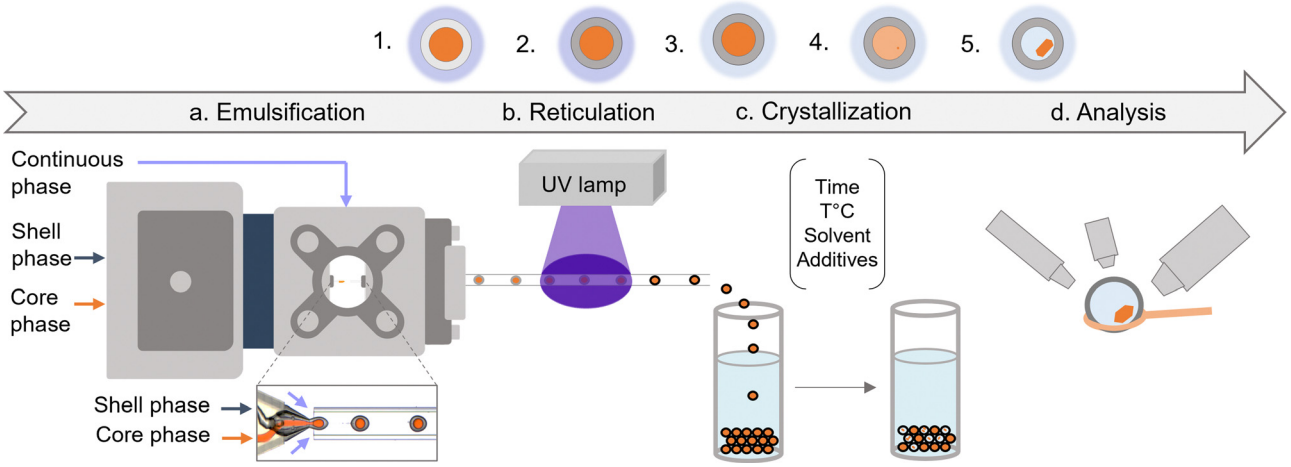

Fig. 1 Schematic representation of the crystallization process. (a) Production of the double emulsion; (b) shell reticulation by polymer irradiation; (c) storage of the capsules into the desired solvent or air, eventually leading to crystallization; (d) *in situ* X-Ray diffraction analysis of selected single crystals. Icons 1. to 5. depict the evolution of double emulsion along the production path: (1) Double emulsion after emulsification; (2) Microcapsule after the reticulation of the shell; (3) Microcapsule placed in the collection medium; (4) Nucleation event within the microcapsule upon exchange through the shell; (5) Encapsulated crystal.

casing (Fig. 1). The shear applied by the continuous phase on the jet leaving the nozzle leads to the formation of double emulsions in dripping mode, which are therefore highly monodisperse (See ESI,† Fig. S5).

In the present work, a Raydrop emulsification device was used to produce water in oil in water double emulsions in a controlled manner at a few hundreds of droplets per seconds (Fig. 1a). A glass capillary connected to the outlet of the emulsification device permitted the UV-irradiation of the train of droplets (Fig. 1b). By using a commercial polymethacrylate resin with 0.1 wt% diphenyl(2,4,6-trimethylbenzoyl)phosphine oxide (TPO) as radical-generating photoinitiator and 20 wt% ethyl Acetate as the intermediate phase, *i.e.* the shell phase, reticulation of the shell material yielded mechanically stable microcapsules featuring a liquid core in a matter of seconds.

This simple process permitted us to produce about 2500 of identical microcapsules per minute. Their size was adapted between 237 μm and 309 μm in between experiments but their size coefficient of variation was maintained below 3% within an experiment run. By using an undersaturated solution of the compound to crystallize into the core phase, we obtained similar microcapsules, containing the desired solute. These capsules can easily be handled and transferred into another solvent or air dried (Fig. 1c).

In a first instance, we used sodium chloride (200 g L^{-1}) as solute in the core phase and left the capsules produced slowly dry out at room temperature. NaCl crystals were obtained overnight within virtually all capsules – which were still intact – (Fig. 2) showing that the water solvent could diffuse through the capsules' shells while NaCl could not (or at a significantly slower rate). The concentration in NaCl would gradually increase, eventually reaching supersaturation. As the diffusion phenomenon through the shell is slow, growth was favoured over nucleation, leading to one crystal in most of the capsules. Although most of the crystal's morphology suggest multiple nucleation events, some of them were single crystals as validated by single crystal XRD. The capsules therefore behave as independent nanolitre-scale crystallization vessels.

Alternatively, capsules containing copper(II) sulphate in water (200 g L^{-1}) were collected into various medium (air, water, acetone, methanol, ethanol, 2-propanol, ethyl acetate) and stored at room temperature, 4.5 °C or −18 °C, permitting the screening of various conditions. When stored into water, the capsules retained their blue colour over one week, highlighting the retention of the $CuSO_4$. When ethyl acetate was use as antisolvent and kept tight at room temperature, water diffused out of the capsule while ethyl acetate diffused in, leading to a slow decrease of copper sulphate's solubility in the solvent mixture within the capsules. After two days, single crystals of $CuSO_4{\cdot}5H_2O$ were observed in some capsules (Fig. 2). Likely the equilibrium state remained within the metastable zone of $CuSO_4{\cdot}5H_2O$, as only a few capsules yielded crystals, but most of which were well defined. When the capsules are stored into ethanol, 2-propanol or acetone, the collection solvent diffused through the shell, leading to a contraction of the aqueous phase containing copper(II) sulphate (See ESI,† Fig. S1). Some capsules led to the formation of crystalline aggregates. Besides, the collection bath was left turbid when acetone or 2-propanol was used, suggesting a reaction with the shell. No clear effect of the collection temperature was observed.

Upon drying in air at 4.5 °C, capsules containing a 190 g L^{-1} glycine solution also led to the formation of crystals in most of the capsules. In about 3% of the capsules of the sample, only one crystal was observed. Interestingly, a mixture of two polymorphs, α-glycine and γ-glycine, were obtained repeatedly and confirmed by single-crystal X-Ray diffraction analysis (Fig. 2, see ESI† for XRD data) within the same sample. A screening of collection solvents was also performed, leading mostly to crystalline aggregates.

To investigate this procedure for the crystallization of macromolecules, we adapted conventional procedures for the

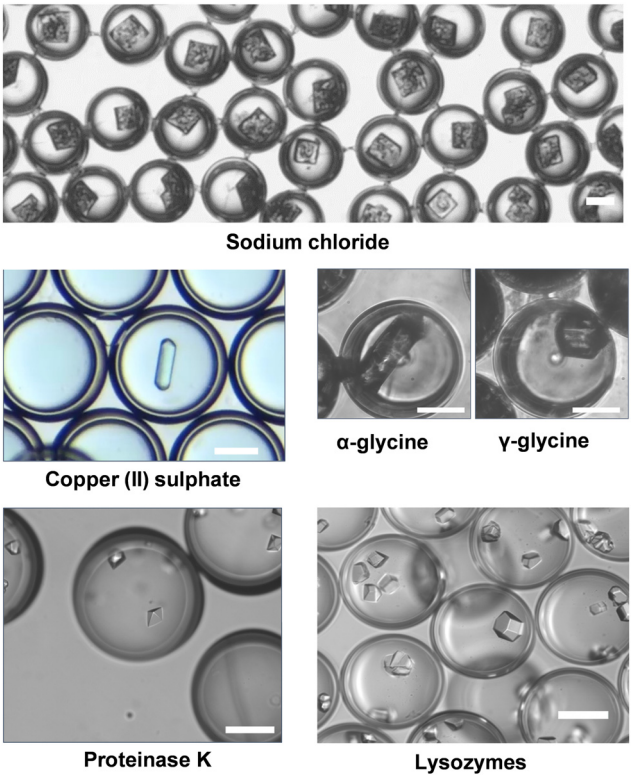

Fig. 2 Examples of encapsulated crystals obtained. Sodium Chloride crystals were obtained with an initial core concentration of 200 g L^{-1} NaCl and appeared upon drying at air; Copper(II) Sulphate crystals were obtained starting from an initial concentration of 200 g L^{-1} $CuSO_4$ with ethyl acetate as collection medium; Glycine crystals were obtained starting from an initial concentration of 190 g L^{-1} and appeared upon drying at air. Both α and γ polymorphic forms have been obtained within the same sample. Proteinase K crystals were obtained starting from a 20 mg mL^{-1} solution of proteinase K with 1.1 M ammonium sulphate at pH 7.0, with 1.2 M ammonium sulphate as collection bath. Lysozymes crystals were obtained starting from a 20 mg mL^{-1} solution of Lysozymes with 5% NaCl at pH 5.0, with a 6% NaCl solution as collection bath. Scale bars are 100 μm.

formation of lysozymes and proteinase K crystals (Fig. 2). In both cases, the protein was solubilized in a saline solution (NaCl 5 wt% for lysozymes and ammonium sulphate 1.1 M for proteinase K). The capsules containing the proteins were then placed into a more concentrated solution of the same salt. After a few days of storage at 4.5 °C, crystals were formed in almost every capsule. Among the hundreds of capsules produced, some contained only one crystal. As NaCl was previously found not to diffuse through the shell, the difference in water activity between inside and outside of the capsules would likely induce its slow diffusion from the inside out by osmosis. The resulting increase in salinity and concentration inside the capsules eventually leads to crystal formation. Encapsulation of lysozyme mainly led to the formation of multiple crystals per capsule, indicating multiple nucleation events. By reducing the salt concentration in the collection bath, the number of capsules containing only one crystal increased, from about none at 20 wt% NaCl to more than 6% at 6 wt% NaCl (Fig. 3) as diffusion would be slower.

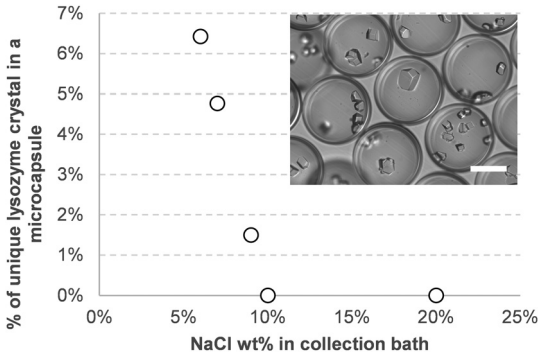

Fig. 3 Percentage of microcapsule containing only one lysozyme crystal, as a function of sodium chloride concentration in the collection bath. Core composition is lysozyme 20 mg mL^{-1}, 5% NaCl, pH 5.0. Storage temperature: 4.5 °C. Inlay picture is of a typical sample, obtained with 6% NaCl as collect bath. Scale bar is 100 μm.

The size of the double emulsion can be modified by adjusting the flow rate of the continuous phase, while the thickness of the shell, for an identical core size, will depend on the flow rate imposed on the shell phase. Therefore, adjusting the shell flowrate during the double emulsion generation permits to control the shell thickness of the capsules. We were able to prepare capsules with shell thicknesses ranging from 25 to 54 μm (See ESI,† Fig. S2 and S3). Samples with capsule shells 36 μm thick and below were found too fragile and neatly broke upon storage (See ESI,† Fig. S4). At 41 μm, invagination of the capsules was observed. The same phenomenon likely occurred and eventually led to breaking with thinner shells.[24] Still, these capsules were unbroken and permitted to obtain glycine crystals when air-dried, yet always several crystals per capsule. At a thickness of 45 μm and above, capsule integrity was maintained throughout storage and between 2.1% and 3.4% of capsules contained only one crystal.

While the shell transparency affords visual inspection of samples for crystals, the low absorption and amorphous nature of the polymethacrylate shell permits the *in situ* X-Ray diffraction data collection directly on the crystals contained in the capsules (Fig. 4). *In situ* data collection at low temperature still needs to be optimized by adjusting conditions for proper cryoprotection. The final quality of the datasets and resulting crystallographic structures were comparable to that of crystals obtained through classical methods (see details in ESI†).

The capsule's shell acts as a porous membrane, that selectively retains the solute but permits solvent exchange. From the

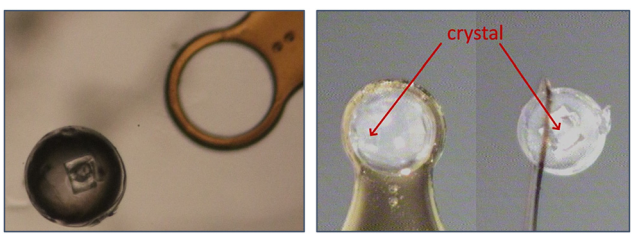

Fig. 4 Picture of a capsule containing a Sodium Chloride crystal on an XRD mounting MicroLoop 300 μm (MiTeGen).

data gathered, all solvents tested - water, ethanol, methanol, 2-propanol, ethyl acetate, acetone, glycerol – diffuse through the capsule shell. On the other hand, salts and macromolecules were found to be kept within the capsules. Likely, the polarity of the firsts and the bulk of the seconds prevent their diffusion within the nonpolar polymethacrylate structure. Glycine being zwitterionic at neutral pH in water, it likely behaves as the salts.

For NaCl and lysozyme crystals, the encapsulation efficiency was close to 100% as virtually no capsule were left empty, with often multiple nucleation events per capsules. On the other hand, $CuSO_4$ with ethyl acetate led to few crystallization events. Likely, in the former scenario, the saturation within the capsules reaches super-solubility limit, leading to crystallization in every capsule, while in the latter, the equilibrium is reached within the metastable zone, leading to more discrete events of nucleation.

This methodology permits to produce thousands of identical yet independent crystallization vessels per minute, each containing as low as 50 ng of solute. As nucleation is a stochastic event,[25] having access to thousands of simultaneous single crystal formation attempts multiplies the chances of success, even though crystallization does not occur within each capsule and/or multiple crystals grow within some, even a 0.1% success rate will statistically yield 10 single crystals alone in their capsule for a sample produced in four minutes. As suggested by the results with glycine, the high number of experiments could also foster the search of polymorphs.

Parameters such as crystallization temperature and collection solvent nature are also easily screened. While it was not performed within the scope of this paper, we expect that varying the nature of the shell polymer could widen the scope of accessible crystallization mechanisms, *e.g.* permitting the use of organic solvents as core phase. A better understanding of the mechanism of transport through the shell opens the way to diffusion of compounds during or after the crystallization to study, for example, complexes by soaking for proteins or inclusion complexes in host guest system.[26]

The possibility to use a gradient of composition during the process of formation of the capsules is a future expansion of the method that could be adapted on the emulsification device used in the present work. Finally, the low size dispersity of the capsules produced could also benefit to serial XRD procedures[27] as they can easily be packed in an hexagonal pattern.

In summary, we demonstrated the possibility to easily produce solid microcapsules which act as independent crystallization vessels for both small molecules and macromolecule. Thousands of parallel experiments can be started within minutes with minimal material consumption. Unlike regular droplets, capsules are mechanically stable and do not need to be maintained confined, allowing their handling and transport, while permitting the *in situ* analysis of the crystals. Although the chosen systems can seem trivial, we believe that this groundwork opens opportunities for the development of integrated methods.

Conceptualization: J.S. and A.D.; investigation M.M., A.D. and N.T.; supervision: A.D., J.W. and J.S; writing – original draft: J.S. wrote the publication; writing – review & editing: all.

Conflicts of interest

The Raydrop device is manufactured and marketed by Secoya Technologies in which A. Dewandre and J. Septavaux hold shares. M. Mettler, N.Tumanov and J. Wouters have no competing interests.

References

1 T. S. Koritsanszky and P. Coppens, *Chem. Rev.*, 2001, **101**, 1583–1628.
2 B. Spingler, S. Schnidrig, T. Todorova and F. Wild, *CrystEngComm*, 2012, **14**, 751–757.
3 N. Calvo Galve, A. Abrishamkar, A. Sorrenti, L. Di Rienzo, M. Satta, M. D'Abramo, E. Coronado, A. J. de Mello, G. Mínguez Espallargas and J. Puigmartí-Luis, *Angew. Chem., Int. Ed.*, 2021, **60**, 15920–15927.
4 D. Rodríguez-San-Miguel, A. Abrishamkar, J. A. R. Navarro, R. Rodriguez-Trujillo, D. B. Amabilino, R. Mas-Ballesté, F. Zamora and J. Puigmartí-Luis, *Chem. Commun.*, 2016, **52**, 9212–9215.
5 B. Rimez, J. Septavaux and B. Scheid, *React. Chem. Eng.*, 2019, **4**, 516–522.
6 F. Bian, L. Sun, L. Cai, Y. Wang, Y. Wang and Y. Zhao, *Small*, 2020, **16**, 1903931.
7 F. D. Giudice, G. D'Avino and P. L. Maffettone, *Lab Chip*, 2021, **21**, 2069–2094.
8 S. Damiati, U. B. Kompella, S. A. Damiati and R. Kodzius, *Genes*, 2018, **9**, 103.
9 Y. Zhang and H.-R. Jiang, *Anal. Chim. Acta*, 2016, **914**, 7–16.
10 N. Candoni, R. Grossier, M. Lagaize and S. Veesler, *Annu. Rev. Chem. Biomol. Eng.*, 2019, **10**, 59–83.
11 D. Velasco, E. Tumarkin and E. Kumacheva, *Small*, 2012, **8**, 1633–1642.
12 D. J. Eastburn, Y. Huang, M. Pellegrino, A. Sciambi, L. J. Ptáček and A. R. Abate, *Nucleic Acids Res.*, 2015, **43**, e86.
13 Y.-J. Eun, A. S. Utada, M. F. Copeland, S. Takeuchi and D. B. Weibel, *ACS Chem. Biol.*, 2011, **6**, 260–266.
14 C. L. Hansen, E. Skordalakes, J. M. Berger and S. R. Quake, *Proc. Natl. Acad. Sci. U. S. A.*, 2002, **99**, 16531–16536.
15 J. Leng and J.-B. Salmon, *Lab Chip*, 2009, **9**, 24–34.
16 J. Ferreira, F. Castro, F. Rocha and S. Kuhn, *Chem. Eng. Sci.*, 2018, **191**, 232–244.
17 A. R. Tyler, R. Ragbirsingh, C. J. McMonagle, P. G. Waddell, S. E. Heaps, J. W. Steed, P. Thaw, M. J. Hall and M. R. Probert, *Chemistry*, 2020, **6**, 1755–1765.
18 A. S. Utada, E. Lorenceau, D. R. Link, P. D. Kaplan, H. A. Stone and D. A. Weitz, *Science*, 2005, **308**, 537–541.
19 R. Seemann, M. Brinkmann, T. Pfohl and S. Herminghaus, *Rep. Prog. Phys.*, 2012, **75**, 016601.
20 T. Fu, Y. Wu, Y. Ma and H. Z. Li, *Chem. Eng. Sci.*, 2012, **84**, 207–217.
21 F. Stauffer, B. Peter, H. Alem, D. Funfschilling, N. Dumas, C. A. Serra and T. Roques-Carmes, *Chem. Eng. Process.*, 2019, **146**, 107685.
22 A. S. Utada, E. Lorenceau, D. R. Link, P. D. Kaplan, H. A. Stone and D. A. Weitz, *Science*, 2005, **308**, 537–541.
23 A. Dewandre, J. Rivero-Rodriguez, Y. Vitry, B. Sobac and B. Scheid, *Sci. Rep.*, 2020, **10**, 21616.
24 F. Boulogne, F. Giorgiutti-Dauphiné and L. Pauchard, *Soft Matter*, 2012, **9**, 750–757.
25 G. M. Maggioni and M. Mazzotti, *Faraday Discuss.*, 2015, **179**, 359–382.
26 B. Wienen-Schmidt, M. Oebbeke, K. Ngo, A. Heine and G. Klebe, *ChemMedChem*, 2021, **16**, 292–300.
27 G. Babnigg, D. Sherrell, Y. Kim, J. L. Johnson, B. Nocek, K. Tan, D. Axford, H. Li, L. Bigelow, L. Welk, M. Endres, R. L. Owen and A. Joachimiak, *Acta Crystallogr., Sect. D: Struct. Biol.*, 2022, **78**, 997–1009.

